# Anisotropic Elastic Properties of Cellulose Measured Using Inelastic X-ray Scattering

**Imke Diddens,[†] Bridget Murphy,[†] Michael Krisch,[‡] and Martin Müller*[,†,§]**

*Institut für Experimentelle and Angewandte Physik, Christian-Albrechts-Universität zu Kiel, D-24098 Kiel, Germany, and European Synchrotron Radiation Facility, BP 220, F-38043 Grenoble Cedex, France*

*Received August 6, 2008; Revised Manuscript Received October 24, 2008*

ABSTRACT: Plant fibers such as linen are remarkably stiff materials in the longitudinal direction of the fiber. As plant cell walls are composites made of cellulose nanocrystals, the so-called microfibrils, embedded in a disordered matrix, those nanocrystals should exhibit an even higher elastic modulus $G$. We have determined the elastic properties of cellulose microfibrils via the sound velocities measured by inelastic X-ray scattering (IXS). The IXS technique is particularly sensitive to crystal properties by discriminating the contribution of disordered material. A strong anisotropy is observed, with a much lower elastic modulus perpendicular to the fiber direction ($G_1 = 15$ GPa) than parallel to it ($G_2 = 220$ GPa). The latter modulus is considerably higher than all values previously determined and will have a significant impact on models for the elastic properties of cellulose microfibrils and of composites based on them.

## 1. Introduction

Cellulose is the most abundant biopolymer on earth and the main building material of plant cell walls. It is a chainlike biopolymer, which during biosynthesis tends to crystallize into stiff, fibrillar nanocrystals, the so-called microfibrils.[1] Those are embedded in a softer matrix of disordered cellulose, other polysaccharides (hemicelluloses), and in woody species, lignin.[2] The understanding of the unique mechanical properties of cellulosic materials such as native cellulose fibers (the Young's modulus of linen can be as high as that of Kevlar, an artificial high-performance fiber) or wood (which provides a specific strength higher than the one of steel) is thus only possible taking into account their composite nature. In order to fully understand and model the mechanical properties of plant cell walls, those of the stiff particles, the crystalline microfibrils, are of utmost importance. A more precise knowledge of the elastic constants of crystalline cellulose will have a major impact on the understanding of the plant cell wall composite as it will in turn allow determining the mechanical properties of the disordered matrix (as a term for all disordered material at the surface of and in between microfibrils) with much higher accuracy than presently possible. In the cell wall architecture, the matrix plays a most crucial role; its properties are e.g. very sensitive to moisture, which strongly influences the mechanical properties of cellulose fibers and wood[3,4] even though the crystalline cellulose microfibrils are not influenced by the adsorbed water.[5]

Cellulose microfibrils in bast fibers such as flax (linen) and ramie have the monoclinic cellulose I $\beta$ structure[6] predominant in higher plants and have a typical diameter of 4−6 nm and a length of about 0.1 $\mu$m.[2] They are highly oriented along the molecular axis (crystallographic $c$-axis, Figure 1) of the molecules parallel to the macroscopic fiber axis.[8] In such a material with fiber texture, even the disordered cellulose molecules are well aligned with the longitudinal fiber axis,[9] further contributing to the fiber's high Young's modulus and strength. Because of their small size, microfibrils cannot be mechanically tested individually, but only inside the composite. The overall mechanical properties are then determined by the stress transfer properties of the embedding matrix. A unique way of studying the mechanical behavior of the material and of the cellulose microfibrils simultaneously is provided by the in situ combination of tensile tests experiments with X-ray diffraction. The local strain of the microfibrils' crystal lattice is measured by a shift of the corresponding Bragg reflections (Figure 1). Mainly the lattice strain in the tensile force direction, i.e., along the fiber axis ($c$), is evaluated;[10−14] however, the study of the Poisson effect in lateral direction (mainly along $a$ as the most compressible direction because of weak van der Waals bonds) is possible as well.[14−17] In the fiber direction, strain inside the cellulose crystals is usually found to be a factor of 3−5 smaller than the macroscopic fiber strain. The calculation of the microfibril Young's modulus requires further knowledge of the stress distribution in the composite and of its morphology. The small lateral microfibril dimensions result in a substantial contribution of surface chains with different molecular conformation from the crystal core.[18] Furthermore, the microfibril orientation distribution depends on the tensile load, implying a contribution of shear deformation.[19] Thus, the published values for the elastic modulus in the $c$-direction (130,[10] ≈128,[11] 136,[12] 90,[13] and 105 GPa)[14] are based on stress distribution assumptions that are

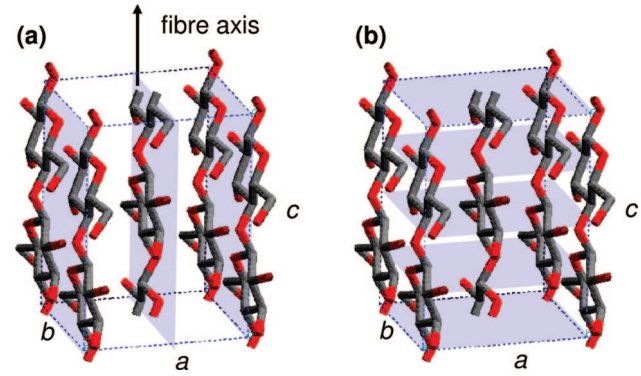


**Figure 1.** Crystal structure of native cellulose[6] (hydrogen atoms are not shown). The cellulose molecules are organized in hydrogen-bonded sheets in the $bc$ plane, whereas between these layers only van der Waals interactions are present. (a) shows the crystallographic 200 lattice planes and (b) the 004 planes (axis settings according to ref 7). For microfibrils in native cellulose fibers with fiber texture, $c$ is the fiber axis.

* Corresponding author: e-mail martin.mueller@gkss.de.
[†] Christian-Albrechts-Universität zu Kiel.
[‡] European Synchrotron Radiation Facility.
[§] Now at GKSS Forschungszentrum Geesthacht, Max-Planck-Str. 1, 21502 Geesthacht, Germany.

10.1021/ma801796u CCC: $40.75 
Published on Web 11/21/2008

difficult to prove. Similar problems occur when band shifts in Raman scattering experiments are interpreted in terms of the elastic modulus (143 GPa).[20] Theoretical values for the axial elastic modulus of cellulose crystals vary with the force field used in the calculations (167.5,[21] 148,[22] and 150 GPa).[23] In summary, reported values for the longitudinal Young's modulus of crystalline cellulose I $\beta$ range from 90 to 170 GPa, a variation in disagreement with the observed structural uniformity.[2]

The present article introduces a novel method for the determination of the elastic moduli of nanocrystals in fibers. Using the inelastic X-ray scattering (IXS) technique, the elastic constants are obtained via the sound velocity as given by the slope of the measured acoustic phonon dispersion relation in the continuum (long-wavelength) limit close to the center of the Brillouin zone, using Christoffel's equation.[24] Even though the cellulose fiber is a composite with amorphous regions, IXS is much less sensitive to the contributions of disordered molecules with respect to those of crystals. In this sense, the technique shows the same selectivity as X-ray diffraction (see above), complementing macroscopic measurements of the sound velocity, which have been used for a long time in determining the macroscopic elastic properties of fibers.[25]

The "classical" method for measuring a phonon dispersion relation is inelastic neutron scattering (INS), which has been carried out earlier on flax fibers to yield generalized phonon densities of states.[9] However, INS does not allow for a determination of the longitudinal velocity of sound at small momentum transfers, $Q$, due to kinematic limitations. In contrast, these limitations do not exist for X-rays with their high incident photon energy of typically 15−20 keV. The relevant energy-momentum transfer region can thus be easily accessed, which is of particular advantage for the investigation of polycrystalline and textured materials,[26−28] including DNA fibers.[27] An IXS experiment on oriented fibers may additionally provide directional sensitivity: parallel fiber bundles can be measured in two orientations, with the scattering vector perpendicular (vertical fibers) and parallel (horizontal fibers) to the crystal $c$-axis. In the first case, scattering from phonon modes involving predominantly motions in the direction of the cellulose chains ($c$-axis, see Figure 1) is suppressed, as already proven in INS experiments.[9]

Here we will demonstrate the potential of IXS for the determination of the anisotropic elastic constants of nanocrystals in fibers by the example of flax fibers. The experimental setup is described in the following section, followed by a summary of the results and their discussion in the framework of the elastic constants of cellulose, and conclusions.

## 2. Experimental Section

In the IXS experiments, industrially bleached flax fibers from the same batch as in previous experiments[8,9,19] were used. The sample consisted of several bundles of flax fibers aligned in a parallel fashion. The bundle orientation was checked beforehand on a larger sample by X-ray fiber diffraction in the laboratory in Kiel using an 18 kW rotating anode with Si(111) monochromator selecting the characteristic Cu K$\alpha_1$ radiation of wavelength $\lambda$ = 0.154 056 nm. Beam size was 0.1 × 1 mm$^2$; the two-dimensional diffraction diagrams (taken with a Photonics Science image-intensified CCD detector) from 13 individual positions on the sample were averaged to yield the fiber diffraction pattern shown in Figure 2. (A similar average was achieved in the IXS experiments; see below.) The azimuthal width of the strong equatorial 200 reflections was determined to 17.5°. This value is larger than the intrinsic microfibril orientation distribution in a single flax fiber of only 7° due to a nonperfect alignment of the individual fibers in the bundles.[8]

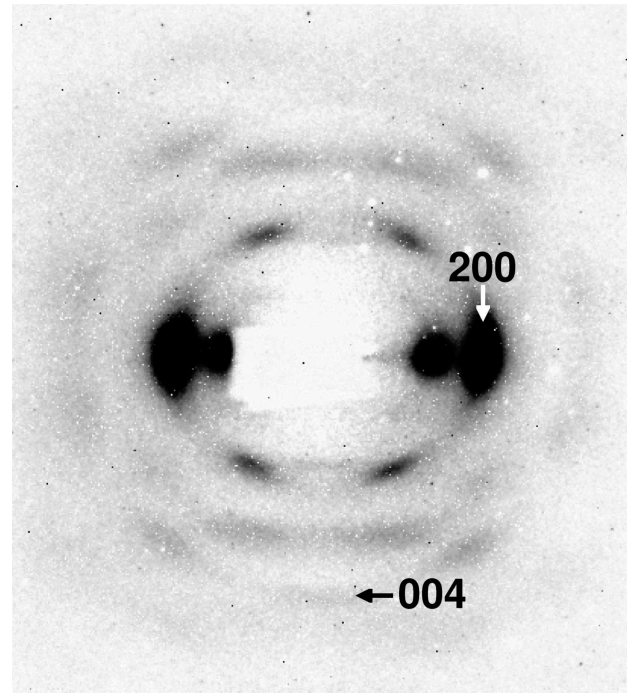


**Figure 2.** Fiber diffraction pattern of a 0.5 mm thick flax fiber bundle (fiber axis was vertical) recorded at a laboratory X-ray source. The scattering signals from 13 different positions on the bundle (exposure time 10 min each) were averaged in order to yield a representative pattern in terms of fiber orientation. The equatorial 200 and the meridional 004 reflections (arrows) correspond to the lattice planes in parts a and b of Figure 1, respectively.

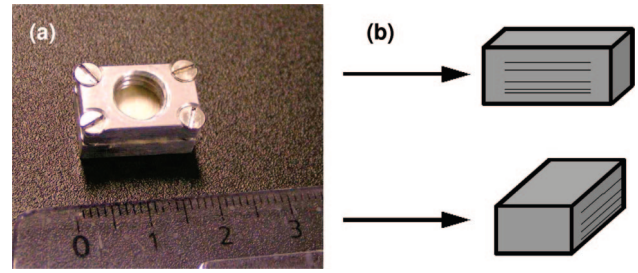


**Figure 3.** (a) IXS sample with oriented flax fibers in an aluminum frame. (b) Oriented fibers were measured with the X-ray beam almost parallel (top, orientation 1) and perpendicular (bottom, orientation 2) to the fiber axis.

The IXS experiment was carried out using beamline ID28 at the European Synchrotron Radiation Facility (ESRF, Grenoble, France). We used the Si(11,11,11) backscattering reflection of the monochromator (energy 21.747 keV) and the analyzers with an overall instrumental energy resolution of ≈1.5 meV. The beam size at the sample position was 250 × 80 $\mu$m$^2$. Sample size was 0.5 × 10 × 10 mm$^3$ with oriented fibers mounted in an aluminum support frame (Figure 3a). The horizontal scattering plane coincides with the plane of the cellulose fibers such that the X-ray beam penetrated about 10 mm of sample in order to yield a sufficiently intense scattering signal. Mounting the sample inside the ID28 standard vacuum chamber minimized air scattering and eliminated the influence of adsorbed water on the spectra taken. The oriented fibers were measured in two orientations (Figure 3b) with the scattering vector $\vec{Q}$ perpendicular (orientation 1; fiber direction almost along the X-ray beam) and parallel (orientation 2; fibers almost perpendicular to the beam) to the longitudinal fiber axis. In the first case, scattering from phonon modes involving predominantly motions in the direction of the molecular chains ($c$-axis) is suppressed. In contrast, in the second orientation, only those modes contribute. In the two orientations, IXS spectra were recorded at 20 different $Q$ values (four analyzer settings for each orientation, $\Delta Q$ = 1.5 nm$^{-1}$). The

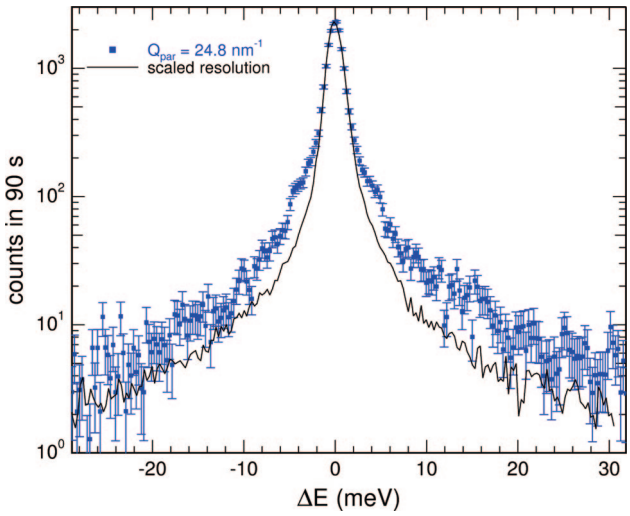


**Figure 4.** IXS spectrum of flax fibers in orientation 2 at $Q = 24.8$ nm$^{-1}$, close to the 004 reciprocal lattice point (blue data points). Please note the logarithmic scale. The elastic line is so strong that phonon frequencies can only be determined from spectra with the elastic line subtracted (black line: experimental resolution function for the same analyzer, scaled to maximum for comparison).

$Q$ positions cover more than the first two Brillouin zones of cellulose in order to determine the longitudinal acoustic phonon branches.

The measured spectra show very strong contributions of elastic scattering (see Figure 4 for an example; please note the logarithmic intensity scale). This scattering consists of both Bragg and disorder scattering: the Bragg reflections are broadened due to the small crystal size (see Figure 2), the amorphous material gives rise to an underlying background, and the contrast between those two phases results in strong small-angle scattering. In the $Q$ range investigated here, there is continuous elastic scattering visible on the equator.[29] A reliable determination of the measured phonon excitation positions was impossible using the standard fitting routines. We decided to evaluate spectra with the elastic line subtracted instead. The experimental ID28 energy resolution function at the relevant energy, responsible for the elastic line shape, was parametrized with a pseudo-Voigt function. This made it possible to adjust not only the intensity but also the exact position of the elastic line and its width before subtraction from the cellulose spectra. The positions of the excitations could then be extracted from the difference spectra and were averaged between the Stokes and anti-Stokes lines.

## 3. Results and Discussion

Figures 5 and 6 are color-coded two-dimensional interpolated maps of all spectra measured in the respective direction; i.e., a single spectrum such as in Figure 4 would correspond to a vertical section (in that particular case at $Q = 24.8$ nm$^{-1}$). They show the $Q$ dependence of the flax fiber spectra after subtraction of the strong elastic line (subtraction artifacts occur in the lighter area around zero energy transfer $\Delta E$) and on a logarithmic intensity scale for the two fiber orientations. In the case of orientation 2 ($Q$ along $c$, Figure 5), only very few spectra around the reciprocal lattice points 002 and particularly around 004 contain significant inelastic intensity. In contrast, for orientation 1 with $Q$ perpendicular to $c$ but—due to the fiber texture—random orientation with respect to $a$ and $b$ comparably well-defined excitations are observed over the whole $Q$ range covered. We shall discuss the analysis of these spectra first.

A striking feature of the two-dimensional representation (Figure 6) is the clear periodicity of the spectra in $Q$. The period apparently corresponds to the wave vector transfer of the most intense equatorial reflection 200 (see Figure 2). 200 is the first $h$00 reflection with a significant structure factor. In the corresponding first Brillouin zone, essentially the longitudinal acoustic phonon branches contribute to the IXS signal.[28] Beyond the first zone, transversal modes may contribute as well, and the overall shape of the measured spectra should approximate dispersionless feature originating from the phonon density of states.[30] It is thus not surprising that in the second and the first half of the third Brillouin zone the excitations are much less well-defined, even though—at least close to the 200 reflection—some excitations of the longitudinal phonon dispersion are still visible.

In Figure 7 the positions of the phonon excitations are plotted. Because of the low intensities, some energies, in particular in

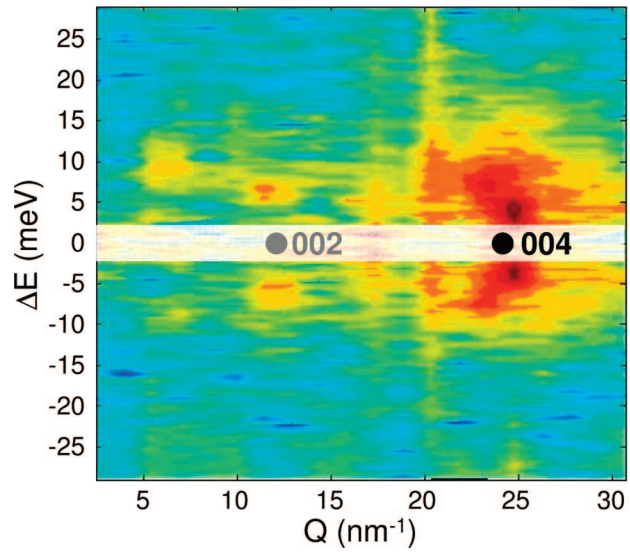


**Figure 5.** $Q$ dependence of inelastic X-ray spectra of oriented flax fibers with $Q$ along [00$l$] (orientation 2) on a logarithmic intensity scale (dark blue: lowest; red: highest intensity). The shaded area for energy transfer $|\Delta E| \leq 2$ meV contains artifacts from the subtraction of the elastic line. The positions of the 002 and 004 reciprocal lattice points are shown; they correspond to meridional reflections in the fiber diagram (Figure 2).

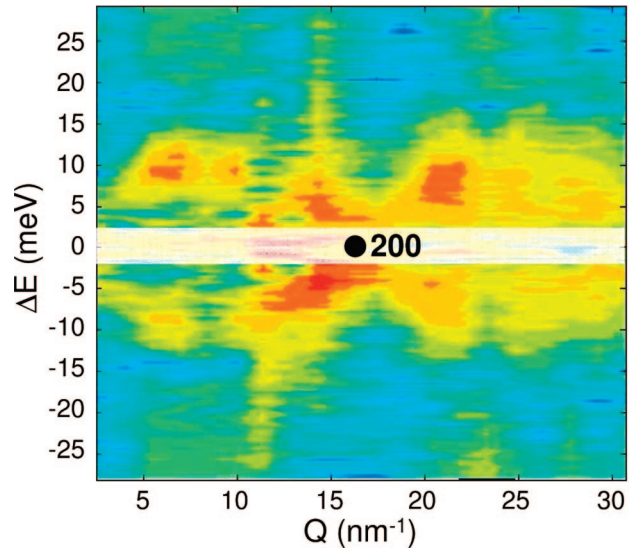


**Figure 6.** $Q$ dependence of inelastic X-ray spectra of oriented flax fibers with $Q$ along [$hk$0] (orientation 1) on a logarithmic intensity scale (dark blue: lowest; red: highest intensity). The shaded area for energy transfer $|\Delta E| \leq 2$ meV contains artifacts from the subtraction of the elastic line. The position of the 200 reciprocal lattice point is shown; it corresponds to an equatorial reflection in the fiber diagram (Figure 2).

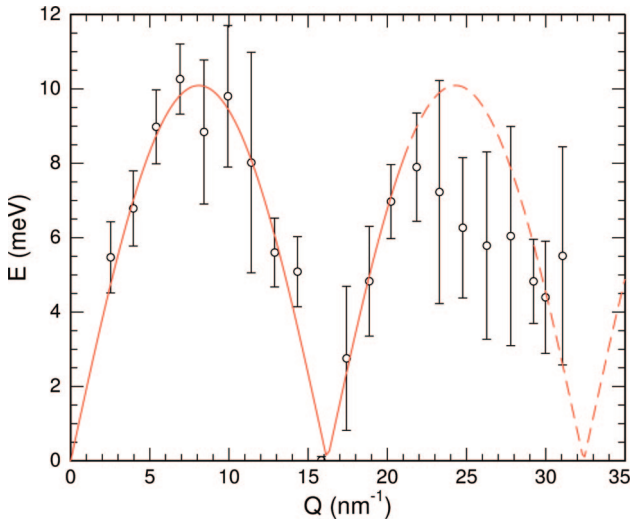


**Figure 7.** Experimental phonon dispersion of native cellulose fibers in orientation 1 in a repeated-zone scheme (circles). The fit with a sine function (eq 1) up to 21 nm$^{-1}$ is shown as a solid line and its extension (not fitted!) by a broken line. The $Q$ value of the equatorial 200 reflection is 16.1 nm$^{-1}$, almost exactly in the center of the second Brillouin zone ($Q$ = 16.2 nm$^{-1}$) as determined in the fit.

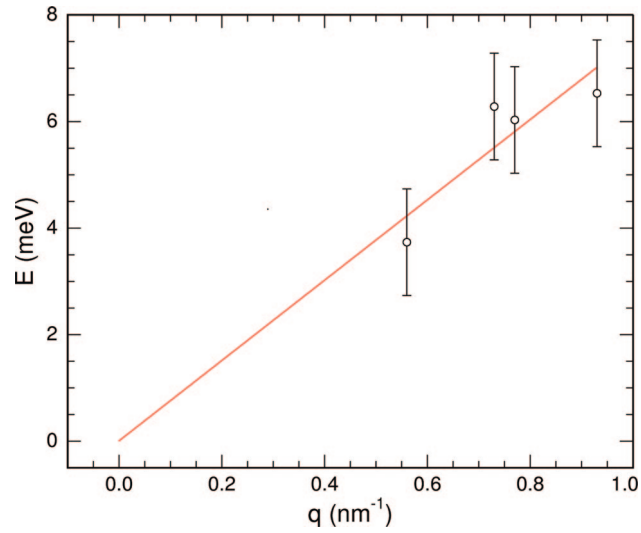


**Figure 8.** Experimental phonon dispersion of native cellulose fibers in orientation 2 in a reduced-zone scheme (circles). The linear fit is shown as a solid line.

the higher Brillouins zones, could only be determined with large errors. The solid line is a fit with the commonly used function

$$E(Q) = \frac{2\hbar}{\pi} v_L Q_{max} \left| \sin\left(\frac{\pi}{2}\frac{Q}{Q_{max}}\right)\right| \quad (1)$$

(where $v_L$ is the longitudinal speed of sound) describing the sinusoidal dispersion of an acoustic phonon branch with periodicity given by $Q_{max}$. One would principally have the choice of either fixing it to a value obtained by approximating the Brillouin zone by a sphere with radius $Q_{max}$ according to the zone volume or to leave it as free parameter in the fit,[31] which we decided to do here. For a reliable determination of the parameter $Q_{max}$ the excitations in the second Brillouin zone (up to 21 nm$^{-1}$) were included in the fit. The resulting $Q_{max}$ = 8.1 ± 0.1 nm$^{-1}$ turns out to be very close to half the expected 16.1 nm$^{-1}$ of the 200 Bragg reflection. Considering the high structure factor of the 200 equatorial cellulose reflection, the phonons that could principally be detected in general [$hk$0] directions (fiber texture) are probably dominated by the [$h$00] contribution. We thus assume that the IXS signal is dominated by a longitudinal acoustic phonon branch along [100]. A sound velocity $v_{L,1}$ = 2973 ± 85 m/s is obtained. The effective elastic modulus $G_1$ (the index in both cases stands for orientation 1) is derived using Christoffel's equation

$$G_1 = \rho_c {v_{L,1}}^2 \quad (2)$$

with the density of crystalline cellulose, $\rho_c$. $\rho_c$ was calculated using the most recent cellulose I $\beta$ crystal structure[6] as 1.676 g/cm$^3$, slightly higher than a value given by Krässig[32] (1.625 g/cm$^3$). With the first value, $G_1$ = 14.8 ± 0.8 GPa is calculated.

This transverse elastic modulus $G_1$ of crystalline cellulose, determined here for the first time experimentally, is supposed to be dominated by the [$h$00] direction (see above) where the cellulose molecules sheets are only weakly van der Waals bonded. Calculations gave a transverse modulus of about 10 GPa,[12] indicating that the [$h$00] direction is the least stiff one of a cellulose crystal. The agreement with our result is good.

In the other orientation (2), which is for measuring phonons along the fiber axis, the phonon intensity is significant only close to the meridional reflections 002 and 004 (Figure 5). (Figure 4 is actually a logarithmic plot of a spectrum close to 004, exhibiting a very strong elastic contribution.) A clear periodicity of the pattern is absent. Instead of analyzing the dispersion over several Brillouin zones, we show the excitations close to the Bragg peaks in a reduced zone scheme (Figure 8) where the phonon wave vector $\vec{q} = \vec{Q} - \vec{G}_{00l}$ for $l$ = 2, 4 ($\vec{G}_{hkl}$: reciprocal lattice vector). The four excitations close to 002 and 004 are found on a straight line through the origin (which was included in the fit), yielding a longitudinal (i.e., along the fiber axis, orientation 2) velocity of sound for longitudinal acoustic phonons, $v_{L,2}$. The thus-obtained $v_{L,2}$ = 11 450 ± 1290 m/s can be used to calculate the elastic modulus of cellulose crystals in the fiber direction via eq 2, giving $G_2$ = 220 ± 50 GPa.

The longitudinal modulus of elasticity, $G_2$, determined here is larger than previously measured[10−14] or calculated[21−23] (see Introduction). One should, however, keep in mind that the "classical" X-ray diffraction experiments rather underestimate the mechanical properties of crystalline material as they crucially depend on an as efficient as possible stress transfer mechanism in the composite. Variations of the stress distribution in the complex molecular network of the embedding matrix can e.g. turn the normal Poisson effect of spruce wood cell wall cellulose microfibrils in the native wood cell wall[17] into a negative Poisson effect upon chemical modification (delignification, Kraft pulping) of the cell wall matrix.[16]

The value for the longitudinal sound velocity of cellulose crystals (about 11500 m/s) found in this work is high. Comparing cellulose to other carbon-containing structures, the cellulose sound velocity is close to that of diamond (18 000 m/s).[28] This means that the predominant strong covalent bonds (C−C and C−O) in cellulose are responsible for the high sound speed. It is reflected in the stiffness of the material: the corresponding Young's modulus of cellulose along the fiber direction of 220 GPa even exceeds that of steel.

## 4. Conclusions

The elastic constants of native cellulose crystals as determined here—220 GPa in fiber direction, 15 GPa perpendicular to the sheets of cellulose molecules—constitute an important step toward a more exact determination of the mechanical properties of cellulose. The elastic modulus in fiber direction is significantly higher than all previously reported values. The observed elastic anisotropy by a factor of 15 reflects the different bonding

systems in different crystallographic directions: covalent bonds in *c*-direction, van der Waals forces along *a*.

In general, the inelastic X-ray scattering technique as presented here is free from artifacts, which in X-ray diffraction experiments would arise from details of the stress transfer between matrix and crystals in plant cell walls. IXS thus does not underestimate the elastic moduli and provides a much more direct access to the elastic properties of nanocrystals in composite materials. Further systematic experiments are on the way in order to investigate the impact of the degree of orientation of fibers, of a possible double orientation in the crystallographic texture,[6] or of the crystal size on the IXS spectra.

**Acknowledgment.** The authors thank Alexei Bosak and Irmengard Fischer (ID28, ESRF) for help with the experiment and data analysis, respectively.

## References and Notes

(1) Cousins, S. K.; Brown, R. M., Jr. *Polymer* **1995**, *36*, 3885–3888.
(2) O'Sullivan, A. C. *Cellulose* **1997**, *4*, 173–207.
(3) Skaar, C. *Wood-Water Relations*; Springer: Berlin, 1988.
(4) Grotkopp, I. Ph.D. Thesis, Christian-Albrechts-Universität zu Kiel, 2006, http://eldiss.uni-kiel.de/macau/receive/dissertation_diss_1838.
(5) Ioelovitch, M.; Gordeev, M. *Acta Polym.* **1994**, *45*, 121–123.
(6) Nishiyama, Y.; Langan, P.; Chanzy, H. *J. Am. Chem. Soc.* **2002**, *124*, 9074–9082.
(7) Sarko, A.; Muggli, M. *Macromolecules* **1974**, *7*, 486–494.
(8) Müller, M.; Czihak, C.; Vogl, G.; Fratzl, P.; Schober, H.; Riekel, C. *Macromolecules* **1998**, *31*, 3953–3957.
(9) Müller, M.; Czihak, C.; Schober, H.; Nishiyama, Y.; Vogl, G. *Macromolecules* **2000**, *33*, 1834–1840.
(10) Sakurada, I.; Ito, T.; Nakamae, K. *Makromol. Chem.* **1964**, *75*, 1–10.
(11) Matsuo, M.; Sawatari, C.; Iwai, Y.; Ozaki, F. *Macromolecules* **1990**, *23*, 3266–3275.
(12) Nishino, T.; Takano, K.; Nakamae, K. *J. Polym. Sci., Part B: Polym. Phys.* **1995**, *33*, 1647–1651.
(13) Ishikawa, A.; Okano, T.; Sugiyama, J. *Polymer* **1997**, *38*, 463–468.
(14) Kölln, K. Ph.D. Thesis, Mathematisch-Naturwissenschaftliche Fakultät der Christian-Albrechts-Universität zu Kiel, Kiel, 2004, http://e-diss.uni-kiel.de/diss_1173.
(15) Nakamura, K.; Wada, M.; Kuga, S.; Okano, T. *J. Polym. Sci., Polym. Phys.* **2004**, *42*, 1206–1211.
(16) Peura, M.; Grotkopp, I.; Lemke, H.; Vikkula, A.; Laine, J.; Müller, M.; Serimaa, R. *Biomacromolecules* **2006**, *5*, 1521–1528.
(17) Peura, M.; Kölln, K.; Grotkopp, I.; Saranpää, P.; Müller, M.; Serimaa, R. *Wood Sci. Technol.* **2007**, *41*, 565–583.
(18) Newman, R. H.; Ha, M.-A.; Melton, L. D. *J. Agric. Food Chem.* **1994**, *42*, 1402–1406.
(19) Kölln, K.; Grotkopp, I.; Burghammer, M.; Roth, S. V.; Funari, S. S.; Dommach, M.; Müller, M. *J. Synchrotron Radiat.* **2005**, *12*, 739–744.
(20) Šturcová, A.; Davies, G. R.; Eichhorn, S. J. *Biomacromolecules* **2005**, *6*, 1055–1061.
(21) Tashiro, K.; Kobayashi, M. *Polymer* **1991**, *32*, 1516–1526.
(22) Marhöfer, R. J.; Reiling, S.; Brickmann, J. *Ber. Bunsen-Ges. Phys. Chem.* **1996**, *100*, 1350–1354.
(23) Eichhorn, S. J.; Davies, G. R. *Cellulose* **2006**, *13*, 291–307.
(24) Auld, B. A. *Acoustic Fields and Waves in Solids*; Wiley: New York, 1973; Vol. *1*.
(25) Ballou, J.; Silverman, S. *Text. Res. J.* **1944**, *14*, 282–292.
(26) Baumert, J.; Gutt, C.; Krisch, M.; Requardt, H.; Müller, M.; Tse, J. S.; Klug, D. D.; Press, W. *Phys. Rev. B* **2005**, *72*, 054302.
(27) Krisch, M.; Mermet, A.; Grimm, H.; Forsyth, V. T.; Rupprecht, A. *Phys. Rev. E* **2006**, *73*, 061909.
(28) Bosak, A.; Krisch, M.; Fischer, I.; Huotari, S.; Monaco, G. *Phys. Rev. B* **2007**, *75*, 064106.
(29) Müller, M.; Czihak, C.; Burghammer, M.; Riekel, C. *J. Appl. Crystallogr.* **2000**, *33*, 817–819.
(30) Bosak, A.; Krisch, M. *Phys. Rev. B* **2005**, *72*, 244305.
(31) Antonangeli, D.; Krisch, M.; Fiquet, G.; Farber, D.; Aracne, C.; Badro, J.; Occelli, F.; Requardt, H. *Phys. Rev. Lett.* **2004**, *93*, 215505.
(32) Krässig, H. A. *Cellulose: Structure, Accessibility and Reactivity*; Gordon and Breach Science Publishers: Yverdon, 1993; Vol. *11*.

MA801796U